THE JOURNAL OF BIOLOGICAL CHEMISTRY VOL. 283, NO. 32, pp. 22222–22232, August 8, 2008

Connection Domain Mutations N348I and A360V in HIV-1 Reverse Transcriptase Enhance Resistance to 3′-Azido-3′-deoxythymidine through Both RNase H-dependent and -independent Mechanisms*[S]

Received for publication, May 8, 2008 Published, JBC Papers in Press, June 10, 2008, DOI 10.1074/jbc.M803521200

Maryam Ehteshami[‡1], Greg L. Beilhartz[‡1], Brian J. Scarth[‡1,2], Egor P. Tchesnokov[‡], Suzanne McCormick[‡], Brian Wynhoven[§], P. Richard Harrigan[§], and Matthias Götte[‡3]

From the [‡]Department of Microbiology and Immunology, McGill University, Montreal, Quebec H3A 2B4, Canada and the [§]B.C. Centre for Excellence in HIV/AIDS, St. Paul's Hospital, Vancouver, British Columbia V6Z 1Y6, Canada

Thymidine analogue-associated mutations (TAMs) in reverse transcriptase (RT) of the human immunodeficiency virus type 1 (HIV-1) cause resistance to 3′-azido-3′-deoxythymidine (AZT) through excision of the incorporated monophosphate. Mutations in the connection domain of HIV-1 RT can augment AZT resistance. It has been suggested that these mutations compromise RNase H cleavage, providing more time for AZT excision to occur. However, the underlying mechanism remains elusive. Here, we focused on connection mutations N348I and A360V that are frequently observed in clinical samples of treatment-experienced patients. We show that both N348I and A360V, in combination with TAMs, decrease the efficiency of RNase H cleavage and increase excision of AZT in the presence of the pyrophosphate donor ATP. The TAMs/N348I/A360V mutant accumulates transiently formed, shorter hybrids that can rebind to RT before the template is irreversibly degraded. These hybrids dissociate selectively from the RNase H-competent complex, whereas binding in the polymerase-competent mode is either not affected with N348I or modestly improved with A360V. Both connection domain mutations can compensate for TAM-mediated deficits in processive DNA synthesis, and experiments with RNase H negative mutant enzymes confirm an RNase H-independent contribution to increased levels of resistance to AZT. Moreover, the combination of diminished RNase H cleavage and increased processivity renders the use of both PP_i and ATP advantageous, whereas classic TAMs solely enhance the ATP-dependent reaction. Taken together, our findings demonstrate that distinct, complementary mechanisms can contribute to higher levels of excision of AZT, which in turn can amplify resistance to this drug.

Human immunodeficiency virus type 1 (HIV-1)[4] replicates using a virally encoded reverse transcriptase (RT), which contains a catalytically active large subunit (p66) and a smaller p66-derived subunit (p51). The p66 subunit comprises the DNA polymerase (residues 1–321), connection (residues 322–440), and RNase H (residues 441–560) domains (1, 2). The RNase H activity, which degrades the RNA of DNA·RNA hybrids, is essentially required to convert the single-stranded viral RNA genome into double-stranded proviral DNA (3).

Due to its key role in viral replication, HIV-1 RT represents a major therapeutic target (4, 5). Approved RT inhibitors belong to two distinct classes: nucleoside analogue and nonnucleoside analogue RT inhibitors (NRTIs and NNRTIs, respectively). NRTIs are synthetic derivatives of the natural deoxynucleosides. The triphosphate forms of NRTIs and cellular dNTPs serve as substrates for HIV-1 RT. In contrast to natural dNTPs, NRTIs lack the 3′-hydroxyl group of the sugar moiety. The incorporated monophosphate (MP) therefore acts as a chain terminator, which prevents phosphodiester bond formation with the next complementary nucleotide (6). NNRTIs are structurally diverse, and members of this family of compounds bind to a hydrophobic pocket (NNRTI-binding pocket) near the polymerase active site to act as allosteric inhibitors by blocking the chemical step (7, 8).

Despite the remarkable progress in the development of potent antivirals, the development of drug resistance, which is associated with viral rebound and treatment failure, remains a problem in the management of HIV infection. Thus, genotypic resistance testing has become an important tool in clinical decision making (9–11). However, since the majority of NRTI and NNRTI resistance mutations are clustered around the polymerase active site and the adjacent NNRTI-binding pocket, respectively (12–14), routine testing involves only the first ~300 residues of HIV-1 RT (15). This region includes polymerase domain mutations M41L, D67N, K70R, L210W, T215F/Y, and K219Q/E, which are referred to as thymidine analogue-

* This work was funded by a grant from the Canadian Institutes of Health Research (CIHR) (to M. G.). The costs of publication of this article were defrayed in part by the payment of page charges. This article must therefore be hereby marked "*advertisement*" in accordance with 18 U.S.C. Section 1734 solely to indicate this fact.

⌘ *Author's Choice*—Final version full access.

[S] The on-line version of this article (available at http://www.jbc.org) contains supplemental Figs. S1–S6.

[1] These authors have contributed equally to this work.

[2] Recipient of a predoctoral stipend from the CIHR.

[3] Recipient of a national career award from the CIHR. To whom correspondence should be addressed: McGill University, Dept. of Microbiology and Immunology, Duff Medical Bldg. (D-6), 3775 University St., Montreal, Quebec H3A 2B4, Canada. Tel.: 514-398-1365; Fax: 514-398-7052; E-mail: matthias.gotte@mcgill.ca.

[4] The abbreviations used are: HIV-1, human immunodeficiency virus type 1; RT, reverse transcriptase; TAM, thymidine analogue-associated mutation; NRTI, nucleoside analogue RT inhibitor; NNRTI, nonnucleoside analogue RT inhibitor; AZT, 3′-azido-3′-deoxythymidine; AZT-MP, AZT monophosphate; d4T, 2′,3′-didehydro-2′,3′-dideoxythymidine; WT, wild type; PBS, primer binding site.

associated mutations (TAMs). TAMs emerge under the selective pressure of 3′-azido-3′-deoxythymine (AZT), and 2′,3′-didehydro-2′,3′-dideoxythymidine (d4T). Three or more TAMs confer resistance to literally all available NRTIs, albeit to different degrees (16–18). TAMs were shown to increase the ability of RT to excise AZT-MP from the 3′-end of the primer, which provides a major mechanism for resistance to this class of antiretrovirals (19). The mutant enzyme recruits ATP, a PP_i donor that attacks the incorporated AZT-MP. Several studies have shown that TAMs do not significantly increase AZT-MP excision in the presence of PP_i (19–21).

Recent findings have suggested that mutations in the C-terminal connection and RNase H domains of RT can significantly amplify resistance to AZT (22–27). Most importantly, many of these mutations, including mutations N348I, A360I/V, and A371V, in the connection domain of HIV-1 RT were identified in clinical samples of HIV-infected individuals. In addition, A371V and Q509L in the RNase H domain emerge under the selective pressure of AZT in cell culture (28). The rare G333D/E polymorphisms have been associated with dual resistance to AZT and other NRTIs (29, 30), and few connection mutations, including Y318F and N348I, have been linked to decreased susceptibility to NNRTIs (23, 26, 31). Most mutations in the C-terminal domains of HIV-1 RT increase resistance to AZT in conjunction with classic TAMs.

Nikolenko *et al.* (32) postulated that AZT-mediated chain termination might be permanent when the RT-associated RNase H activity has completely degraded the template strand. Conversely, AZT resistance could be enhanced by diminishing RNase H cleavage, because the increase in the half-life of the RNA template provides more time for excision to occur (32). A recent study on N348I provided evidence to link diminished RNase H cleavage and increased rates of excision (26). However, the underlying mechanism remains elusive. Additionally, RNase H-independent contributions to resistance may not be excluded, although increases in excision were exclusively observed with DNA·RNA substrates and not with DNA·DNA (26).

To address this problem, we have focused on the study of connection domain mutations A360V and N348I. The combined mutations were shown to cause marked increases in resistance to AZT, predominantly when present against a background of TAMs (33). N348I was also shown to confer low level resistance to AZT and NNRTIs in the absence of TAMs (26). A360 is part of the RNase H primer grip motif that interacts with the nucleic acid substrate (34), whereas most other resistance-associated residues in the connection domain are not in contact with the substrate. Here we show that N348I and A360V compromise binding of transiently formed DNA·RNA hybrids selectively in the context of RNase H-competent complexes. Moreover, the mutant enzymes increase processive DNA synthesis and retain their ability to augment excision of AZT-MP against an RNase H-negative background in HIV-1 RT. Thus, connection domain mutations increase AZT resistance through both RNase H-dependent and -independent mechanisms.

EXPERIMENTAL PROCEDURES

Prevalence and Resistance Correlates of Connection Domain Mutations—Amino acid substitutions in the connection domain of HIV-1 RT potentially associated with exposure to antiretroviral therapy were identified by determining the prevalence of substitutions in a total of 4208 individuals in British Columbia, Canada. This included 1606 treatment-naive individuals at the time of genotypic testing. In addition, genotype data from a further 2422 treatment-experienced individuals was available.

Enzymes and Nucleic Acids—Heterodimeric HIV-1 RT (p66 and p51) were expressed and purified as previously described (35). Mutant enzymes were generated through site-directed mutagenesis with the Stratagene QuikChange™ kit using the manufacturer's protocol. "WT RT" refers to the wild type enzyme, and "TAMs" refers to mutants that contain the following amino acid substitutions: M41L, D67N, L210W, and T215Y. This cluster is associated with high levels of resistance to AZT. TAMs/A360V contains in addition to these four changes the A360V connection domain mutation. The same nomenclature is applied to the other mutants used in this study: TAMs/N348I and TAMs/A360V/N348I. TAMs/E478Q and TAMs/A360V/N348I/E478Q are equivalent, RNase H-negative mutants (supplemental Fig. S1*A*). Nucleic acid substrates used in this study were derived from the HIV-1 primer binding site (PBS) region. RNA and DNA oligonucleotides used in this study were chemically synthesized and obtained from Invitrogen (supplemental Fig. S1*B*).

The long RNA template PBS-250 was generated through *in vitro* transcription with T7 RNA polymerase (36). Nucleic acid substrates were ^{32}P-radiolabeled essentially as described previously (37). Briefly, 5′-end labeling was performed with [γ-^{32}P]ATP (PerkinElmer Life Sciences) and T4 polynucleotide kinase (Fermentas). Reactions were allowed to proceed for 1 h at 37 °C. Labeled DNA or RNA was purified on 12% polyacrylamide gels containing 50 mM Tris borate, pH 8.5, 1 mM EDTA, and 7 M urea and then eluted overnight in a buffer containing 500 mM ammonium acetate and 0.1% SDS.

Multisite AZT-MP Excision and DNA Synthesis Assay—20 nM 5′-radiolabeled DNA primer PBS-28 (5′- CTTTCAGGTC-CCTGTTCGGGCGCCACTG-3′) was annealed to a 3-fold molar excess of complementary PBS-250 (as described above). In order to form the DNA·RNA hybrid duplex, the nucleic acid substrates were hybridized, in the presence of 50 mM NaCl and 50 mM Tris-HCl, pH 7.8, by heating at 95 °C for 3 min followed by a gradual decrease to room temperature for 45 min. The hybridized DNA·RNA substrate was then incubated in a buffer containing 50 mM NaCl and Tris-HCl, pH 7.8, 100 μM EDTA, 2 μM of each of the four dNTPs, 2 μM AZT-TP, and 400 nM RT (WT or mutant). Pyrophosphatase-treated ATP was added at a final concentration of 3.5 mM to each sample. 50 μM PP_i was added in PP_i-mediated excision reactions. Incorporation and excision of AZT-MP was initiated by the addition of 6 mM $MgCl_2$ at 37 °C. The reaction was stopped at various time points with 95% formamide containing trace amounts of xylene cyanol and bromphenol blue. Samples were resolved on a 12% polyacrylamide denaturing gel and analyzed with a PhosphorImager

(Amersham Biosciences) using Quantity One and ImageQuant software.

Enzyme Processivity—The reaction mixture was prepared as described above, without the addition of AZT-TP, ATP, or PP_i. To ensure single turnover conditions, DNA synthesis was initiated in the presence of 2 mg/ml heparin (Bioshop) together with 6 mM $MgCl_2$. Reactions were stopped at different time points. The amount of the full-length product (*P*), as well as the amount of the remaining, nonextended substrate (*S*) was measured after 3 h. Also, the total substrate (*TS*) was quantified as represented in the control reaction in the absence of $MgCl_2$. The fraction of competent complex was derived from the term $1 - S/TS$). This represents the fraction of enzyme-substrate complexes available for extension at equilibrium prior to initiation. The fraction of "processive complex" (*i.e.* the complexes that did not dissociate before the enzyme had reached the 5′-end of the template) was derived from the ratio *P*/*TS*. Therefore, the term $(P/TS)/(1 - S/TS)$ or $P/TS - S$ defines enzyme processivity, expressed as percentage of processive complex (see Table 4).

RNase H Activity—The 5′-radiolabeled RNA template was heat-annealed to a 2-fold molar excess of the complementary DNA primer to form the DNA·RNA substrate, as described above. 100 nM of the preformed substrate was incubated with 200 nM RT in a buffer containing 50 mM Tris-HCl, pH 7.8, 50 mM NaCl, and 100 μM EDTA. The reaction was started with 6 mM $MgCl_2$ at 37 °C. RNase H cleavage was monitored over time, with reactions stopped and analyzed as described above.

Band Shift Experiments—50 nM 5′-radiolabeled DNA primer (3′-CACCGCGGGCTTGTCCCTGGA-5′) was annealed to a 2-fold molar excess of a complementary 52-nucleotide RNA template (5′- GGAAAUCUCUAGCAGUGGCGCCCGAACAGGGACCUGAAAGCGAAAGGGAAAC-3′). The hybrid formed consists of a 21-bp double-stranded region with a 17-nucleotide-long overhang at the template 3′-end. As such, it will be referred to as the "21-bp hybrid duplex." The hybrid was incubated with 100 nM WT RT and TAMs/A360V/N348I, respectively, in a buffer containing 50 mM NaCl and 50 mM Tris-HCl, pH 7.8. RNase H cleavage was initiated at 37 °C after the addition of 6 mM $MgCl_2$. Samples were loaded at various time points on a 6% nondenaturing polyacrylamide gel and analyzed as described above.

Single Nucleotide Excision/Rescue Assay—A 5-fold molar excess of RT (250 nM final concentration) was incubated with the 12-bp duplex hybrid containing a purified primer chain-terminated with AZT or d4T, as described (38). 3.5 mM pyrophosphatase-treated ATP, 10 μM dTTP, 10 μM dGTP, and 20 μM ddCTP were also added to monitor rescue of AZT-terminated DNA synthesis. The combined excision of AZT-MP and rescue of DNA synthesis was allowed to proceed at 37 °C over time (up to 90 min). Excision products were separated by 12% polyacrylamide gel electrophoresis. The results were quantified and plotted with Prism 4.0 software using the one-phase exponential association formula.

Substrate Binding—The equilibrium dissociation constant for polymerase-competent complexes ($K_{d(pol)}$) was measured on the basis of published protocols (39, 40). Briefly, the amount of product generated during a single turnover was quantified and plotted *versus* DNA·RNA substrate concentrations. Data points were fitted to the quadratic equation as described (35), which provides $K_{d(pol)}$ values for the active RT·DNA·RNA binary complex. This analysis also determines the maximum concentration of the binary complex that is competent for nucleotide incorporation at saturating concentrations of DNA·RNA substrate, which is equivalent to the concentration of active enzyme. Initial experiments were therefore used to determine the amount of enzyme that was required to generate 150 nM maximum product for wild type and mutants. Briefly, the 5′-radiolabeled DNA primer (5′ AGGTCCCTGTTCGGGCGCCAC-3′) was used to form either a 15-bp hybrid duplex with the RNA template (5′ ggaaaucucuagcaguggcgcccgaacag-3′) or a 21-bp hybrid duplex with RNA template (5′-ggaaaucucuagcaguggcgcccgaacagggacct-3′). The substrate was incubated with RT in a buffer containing 50 mM NaCl, Tris-HCl, pH 7.8, and 100 μM EDTA. The concentration of the substrate ranged from 17 to 1000 nM, and the reaction was initiated by the addition of 6 mM $MgCl_2$, 20 μM dTTP, and 2 mg/ml heparin trap. Samples were incubated at 37 °C for 5 min and analyzed as described above. A similar protocol was applied to measure the equilibrium dissociation constant for RNase H-competent complexes ($K_{d(RNase\ H)}$). In this case, we utilized 5′-end-labeled RNA templates and initiated the reaction in the absence of nucleotide substrate. The data were quantified using ImageQuant 5.2 and analyzed using Prism 4.0.

TABLE 1
Prevalence of mutations in the connection domain of RT in treated and untreated individuals

RT codon	Prevalence (untreated)[a]	Prevalence (treated)[b]	Increase in prevalence
	%	%	%
277	52.93	59.83	6.90
286	27.27	32.72	5.45
288	9.53	14.10	4.57
348	0.80	12.10	11.30
356	19.12	27.18	8.07
358	5.42	10.85	5.43
359	8.90	16.36	7.46
360	21.36	28.82	7.47
371	5.35	12.66	7.31
386	13.26	18.00	4.74

[a] The prevalence (in percentage) of amino acid substitutions in the HIV-1 RT from treatment-naive individuals ($n = 1606$).
[b] Prevalence (percentage) of amino acid substitutions in the HIV-1 RT from treatment-experienced individuals ($n = 2422$).

RESULTS

In Vivo Prevalence of A360V—The *in vivo* prevalence of mutations in the connection domain of RT was studied in a large cohort of individuals from British Columbia, Canada, as a function of exposure to antiretroviral selection pressure. The populations studied included both treatment-experienced ($n = 2422$) and treatment-naive ($n = 1606$) individuals. Several positions in the connection domain, in particular Asn^{348} and Ala^{360}, showed large increases in prevalence of amino acid substitutions in the treatment-experienced population (Table 1). Substitutions at codon 348 increased in prevalence from 0.8% in the untreated population to over 12.1% in the treatment-experienced populations (26), whereas those at position 360 increased in prevalence from 21.4% to over 28.8%, suggesting a significant selective advantage. The increase in prevalence at codon 360

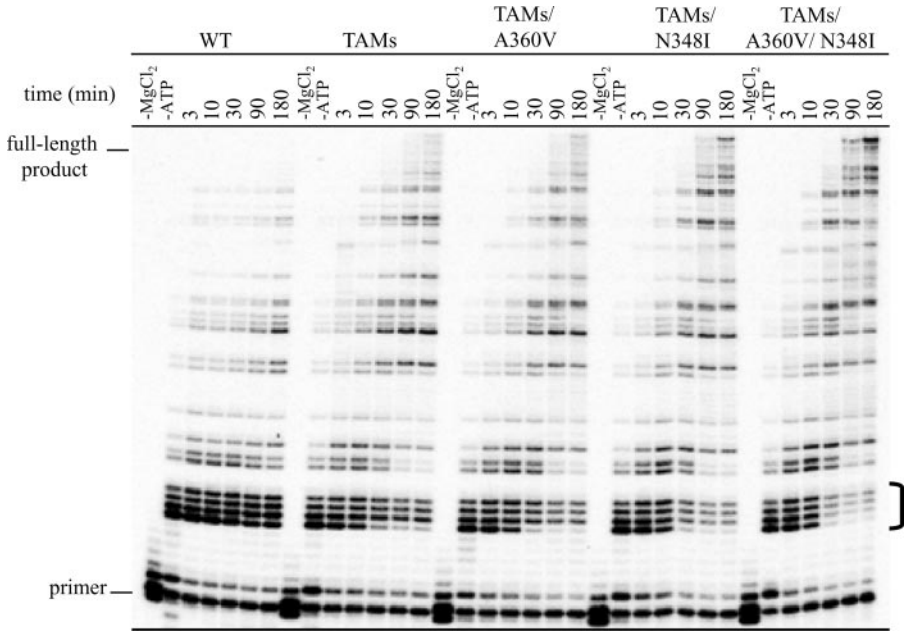

FIGURE 1. **ATP-mediated excision of AZT-MP and rescue of DNA synthesis on a DNA·RNA substrate.** The long DNA·RNA (PBS-28/PBS-250) substrate was employed to assess DNA synthesis rescue over time in the presence of AZT-MP and ATP for each of the RT enzymes (WT, TAMs, TAMs/A360V, TAMs/N348I, and TAMs/A360V/N348I, respectively). The *lowest band* is the radiolabeled DNA primer, and the *highest band* is the full-length DNA product. The *bracket* highlights, as an example, sites of AZT-MP incorporation where DNA synthesis is abrogated. The disappearance of these bands is representative of AZT-MP excision and correlates with increased final DNA product formation. The negative, *−ATP control lane* shows polymerization in the absence of ATP-mediated DNA synthesis rescue. Of note, the amount of product generated with the various enzymes is identical under these conditions.

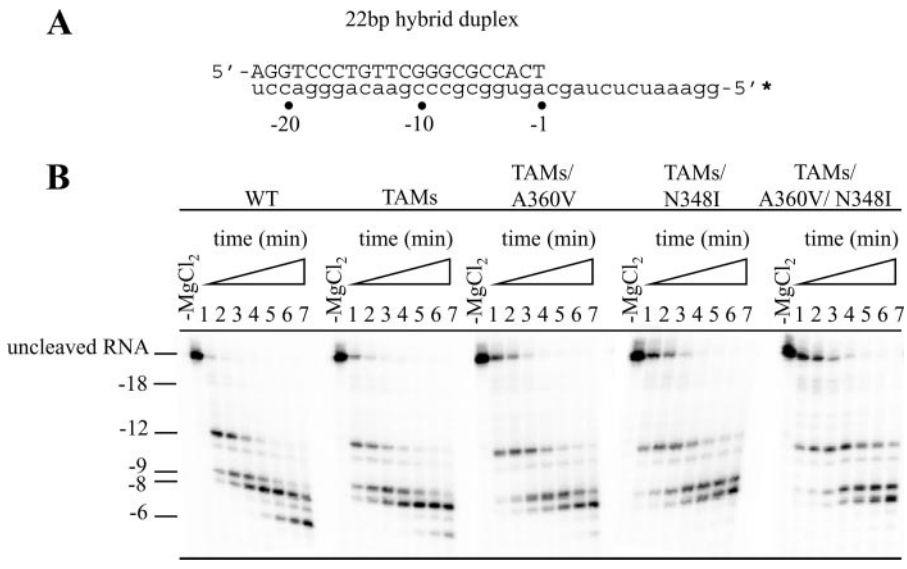

FIGURE 2. **RNase H-mediated RNA template degradation.** *A*, the 22-bp hybrid duplex consists of the DNA primer and the RNA template radiolabeled at the 5′-end (indicated by an *asterisk*). *B*, the DNA·RNA substrate was incubated with the RT enzyme (WT, TAMs, TAMs/A360V, TAMs/N348I, and TAMs/A360V/N348I, respectively). RNase H cleavage was initiated by the addition of $MgCl_2$ at 37 °C and was stopped at 0.5, 1, 2, 4, 8, 12, and 20 min (indicated by *1–7*). The negative, *−$MgCl_2$* control shows the RNA template of the full-length 22-bp hybrid prior to RNase H cleavage. The polymerase-dependent cleavage product at position −18 is rapidly degraded due to high concentrations of RT and is therefore seen only as a faint band in the beginning of the reaction. The accumulating lower bands (*cuts −12* to *−6*) represent the polymerase-independent cleavage products.

was driven in part by a modest increase in the prevalence of a common polymorphism A360T, but predominantly by an increase in the A360V substitution. Like the N348I mutation, A360V was observed in less than 1% of the untreated population ($n = 15$ of 1606) and increased to 8.5% after treatment ($n =$ 205 of 2422). Other mutations (A360I and A360S) were observed only rarely. Furthermore, A360V was highly correlated with various mutations considered to be part of the TAMs cluster; for example, of the samples with A360V, 35% were associated with M41L, 21% with D67N, 30% with K70R, 17% with L210W, 42% with T215Y/F, and 17% with K219Q/E. In contrast, less than 20% of samples with the A360T had TAMs. A360V usually appeared late in therapy, on average 2.5 years after the onset of antiretroviral treatment, and typically appeared after TAMs selection. The A360V mutation appeared in over 120 TAM contexts, but the most common TAM patterns in which it appeared consisted of M41L/215Y or M41L/L210W/T215Y.

Connection Domain Mutations A360V and N348I Increase ATP-mediated Excision on DNA·RNA Substrates—The combination of A360V and N348I, when present against a background of TAMs was shown to amplify resistance to AZT but not to d4T (33). The crucial role played by TAMs suggests that the combination of TAMs and connection domain mutations further increase efficiency of ATP-mediated AZT-MP excision. To address this question directly, we monitored DNA synthesis in the presence of AZT-TP and ATP on a relatively long RNA template that allows polymerization of 185 nucleotides. The reaction covers incorporation and excision of AZT-MP as well as the ensuing rescues of DNA synthesis. The data show that enzymes containing TAMs/A360V and TAMs/N348I, respectively, increased full-length product formation when compared with TAMs (Fig. 1). The efficiency of rescue of DNA synthesis follows the order WT RT < TAMs < TAMs/A360V < TAMs/N348I < TAMs/A360V/N348I.

A360V and N348I Reduce RNase H Activity and Mediate the Accumulation of Truncated Substrates—N348I-containing mutant enzymes were shown to reduce RNase H activity (26, 33). Here, time course experiments were employed to compare RNase H cleavage efficiencies in the context of each of the

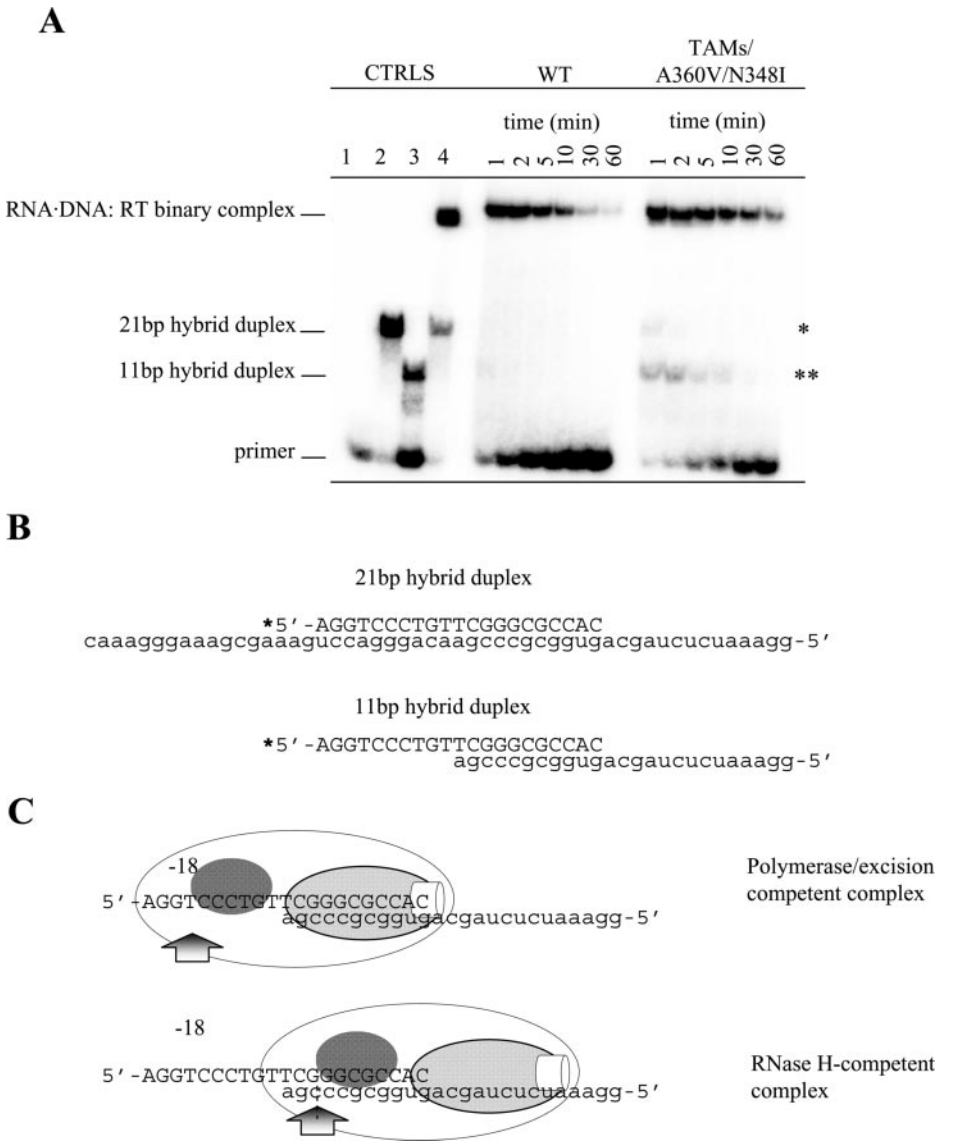

FIGURE 3. **Accumulation of transiently formed hybrids with the TAMs RT containing connection domain mutations A360V and N348I.** *A*, DNA·RNA·RT binary complex formation was monitored in a time course. *Lane 1*, control radiolabeled DNA primer alone. The full-length 21-bp hybrid duplex and the truncated 11-bp hybrid duplex are shown in *lanes 2* and *3*, respectively. A control for complex formation was resolved in the absence of $MgCl_2$ in *lane 4*. *, the full-length hybrid present with the mutant RT. **, the accumulation of the transiently formed hybrid with the TAMs/A360V/N348I RT. *B*, the oligonucleotide sequences for the 21-bp and 11-bp hybrid duplexes are depicted. *C*, when the polymerase active site (*white cylinder*) is occupied by the 3′-end of the DNA primer, the RNase H active site (*arrow*) is positioned ~18 bp upstream. The first 10 nucleotides are in contact with the polymerase region (*gray oval*), whereas some nucleic acid interactions are made through the RNase H primer grip (*darker oval*). This conformation is referred to as polymerase-competent. When the polymerase active site is no longer occupied by the 3′-end of the primer and contacts with the polymerase site are minimized, most substrate enzyme interactions occur through the RNase H primer grip. This conformation is referred to as RNase H-competent. As a consequence, residues of the RNase H primer grip (*e.g.* Ala^{360}) interact with single- or double-stranded regions of the substrate, depending on the conformation of the complex.

mutant enzymes described above. Reactions were monitored on a 5′-end-labeled RNA template (Fig. 2*A*). Deficits in RNase H activity are seen here in both delayed degradation of the full-length substrate and diminished formation of the shorter fragment. This finding suggests that connection mutations affect primary RNase H cuts as well as secondary cuts that occur when the RT enzyme moves in the 3′ to 5′ direction of the template (41–44). The shortest fragment (*i.e.* the cut at position −6) is only seen with WT RT and to a lesser degree with TAMs (Fig. 2*B*). Overall, the efficiency of RNase H cleavage follows the order WT RT > TAMs > TAMs/A360V > TAMs/N348I > TAMs/A360V/N348I, which correlates inversely with the respective efficiencies of excision.

Accumulation of Transiently Formed DNA·RNA Hybrids—As a consequence of the diminished RNase H activity with A360V and N348I, medium sized fragments (*e.g.* fragments with RNase H cuts at positions −12, −9, and −8) accumulate when compared with WT RT that ultimately produces the −6 product (Fig. 2*B*). We then wanted to determine whether the shorter RNA fragments can form stable DNA·RNA hybrids that serve as substrates for the excision reaction. Preformed RT complexes with a 21-bp DNA·RNA hybrid duplex were incubated with Mg^{2+} at different time points to monitor the effect of RNase H cleavage on product formation under nondenaturing conditions (Fig. 3). In this experiment, we compared WT RT with TAMs/A360V/N348I that showed a severe reduction in RNase H cleavage. Our results show an accumulation of transiently formed hybrids with the mutant enzyme (Fig. 3*A*). The corresponding band co-migrates with an 11-bp DNA·RNA duplex that was derived from the original 21-bp substrate (Fig. 3*B*). These data show that the mutant enzyme produces shorter hybrids that dissociate from the complex and accumulate in a short window of time. In contrast, such transiently formed hybrids are hardly seen with WT RT. In this case, RNase H cleavage appears to force the release of the primer at early time points, and the primer does not rebind to the enzyme under these conditions. The release of the primer is less efficient with the mutant enzyme, which provides experimental evidence for the hypothesis that connection domain mutations can delay the irreversible degradation of the DNA·RNA substrate (33).

This experiment also suggests that transiently formed hybrids dissociate from the RT complex before the template is completely degraded. However, the mutant shows an increased rate of excision, which requires rebinding of the shorter substrates. Excision can only occur when the 3′-end of the primer is located at the polymerase active site. In this conformation, the RNase H domain may only cleave the substrate when the hybrid

region contains at least 18 or 19 base pairs, which defines the distance between polymerase and RNase H active sites (Fig. 3*C*, *top*) (34, 42, 44, 45). Shorter templates are not in contact with the RNase H domain. Thus, RNase H cleavage must occur in a different conformation, in which the polymerase active site has released the 3′-end of the primer (Fig. 3*C*, *bottom*). We therefore need to distinguish between polymerase- (or excision)-competent complexes and RNase H-competent complexes, respectively. These complexes are structurally distinct, and connection domain mutations may influence structure and function of RT depending on the particular conformation.

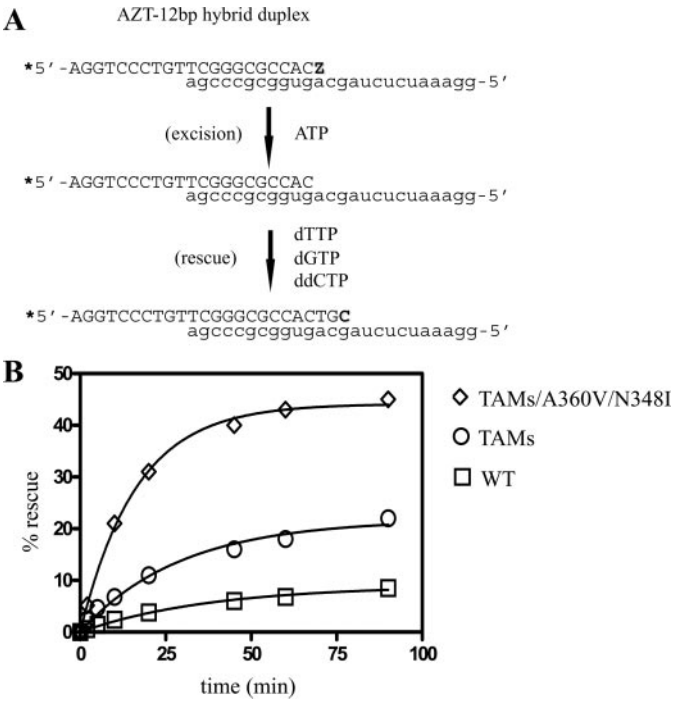

FIGURE 4. **Single-site AZT-MP excision and rescue of DNA synthesis.** *A*, a single-site AZT-MP excision assay was performed on the 12-bp hybrid duplex, which was pre-chain-terminated with AZT (indicated by *Z* at the 3′-terminus of the DNA primer). ATP-mediated excision is followed by DNA synthesis rescue by the addition of the next complementary nucleotide. ddCTP is added to prevent multisite incorporation. *B*, the gel-based excision assay was quantified, and the amount of ATP-mediated rescue product was plotted with respect to time with WT RT (□), TAMs RT (○), and TAMs/A360V/N348I RT (◇). The plot is the average of three separate experiments with minimum R^2 value of 0.98.

To analyze whether the shorter hybrids can serve as substrates for AZT-MP excision and rescue of DNA synthesis, we utilized an AZT-terminated primer that was hybridized with a short RNA fragment to form a 12-bp hybrid duplex (Fig. 4*A*). The efficiency of excision showed the following order in a time course: WT RT < TAMs < TAMs/A360V/N348I (Fig. 4*B*). Thus, connection domain mutations facilitate excision of AZT-MP on short DNA·RNA substrates. DNA·RNA hybrids with a duplex region that is shorter than 8 bp are not used for the combined excision/rescue reaction (supplemental Fig. S2).

When the next complementary nucleotide occupies the active site of RT in the presence of a chain-terminated primer, a dead end complex is formed, and excision is no longer possible (19, 46). D4T-MP was shown to be sensitive to dead end complex formation, whereas AZT-MP compromises binding of the next nucleotide (47). The same result was obtained with the short hybrid substrate, which helps to explain why connection domain mutations N348I and A360V do not amplify resistance to d4T (33) (supplemental Fig. S3).

The Effect of Connection Domain Mutations on Substrate Binding—To determine the effects of connection domain mutations on substrate binding, we measured the equilibrium dissociation constant (K_d) in the context of both polymerase- and RNase H-competent complexes.

A recent study has shown that the connection domain mutation G333D can increase substrate binding under steady-state conditions (29). Our experiments were performed under single turnover conditions to avoid multiple dissociation and reassociation events that complicate the interpretation of the data. We initially determined the minimum length of a DNA·RNA substrate that allowed us to measure K_d values under single turnover conditions and found that RNase H activity could not be reliably quantified when the duplex region is shorter than 16 base pairs (supplemental Fig. S4). To determine the equilibrium dissociation constant of the RNase H- competent complex ($K_{d(\text{RNase H})}$), we monitored RNase H activity for each of the aforementioned mutant enzymes on the 16-bp hybrid substrate (Fig. 5). Substrate binding appears to be slightly compromised (~2-fold) with TAMs ($K_{d(\text{RNase H})}$ of 188.1) when compared with WT RT, which showed a $K_{d(\text{RNase H})}$ value of 104 nM (Table 2). This effect is much more pronounced in the presence of connection mutations. TAMs/A360V showed a moderate 3.6-fold

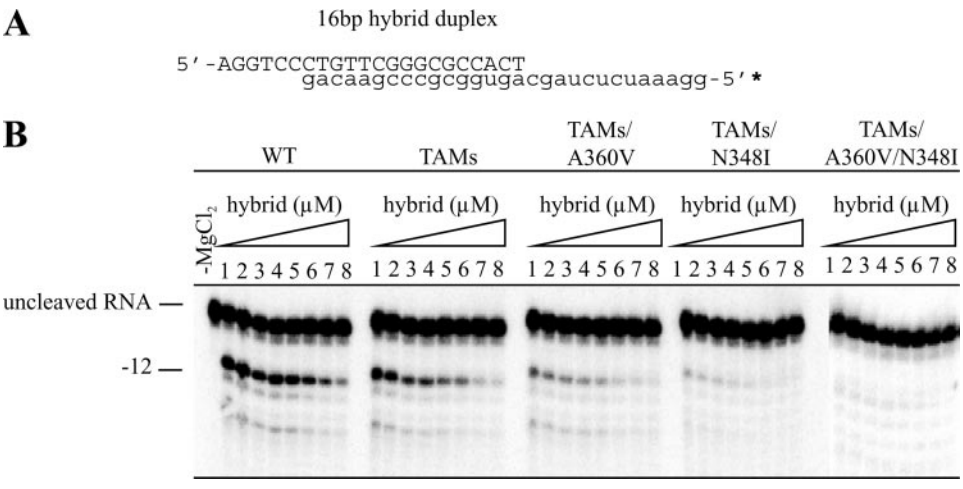

FIGURE 5. **Affinity of RT enzyme for the DNA·RNA substrate in the RNase H-competent complex.** *A*, the 16-bp hybrid duplex consists of the DNA primer and the truncated RNA template radiolabeled at the 5′-end (indicated by an *asterisk*). *B*, RNA degradation was monitored on a polyacrylamide denaturing gel, where the *upper band* is the nondegraded RNA template, and the *lower band* is the cleaved RNA product (*−12*). The 16-bp hybrid duplex concentration gradient is indicated by *1–8*, representing 59, 88, 103, 197, 296, 444, 666, and 1000 nM hybrid duplex, respectively. Quantification of production formation allows for the calculation of $K_{d(\text{RNase H})}$ values (refer to Table 2).

increase in K_d values, TAMs/N348I showed an 8.8-fold increase, and RNase H activity is hardly detectable when both mutations were combined with TAMs.

A similar pattern is seen with a longer substrate that contains the 22-bp hybrid duplex region. However, substrate binding is generally increased when compared with the shorter 16-bp hybrid. Together, the data show that the loss of contacts with the polymerase domain cause severe reductions (5–10-fold) in substrate binding, and this effect is enhanced with the connection domain mutations.

TABLE 2
RNase H-based K_d values

RT enzyme	16-bp hybrid duplex		22-bp hybrid duplex	
	$K_{d(\text{RNase H})}$	FC[a]	$K_{d(\text{RNase H})}$	FC
	nM	*-fold*	*nM*	*-fold*
WT	104 ± 16.7		18.8 ± 7.30	
TAMs	188 ± 84.4	1.81	43.9 ± 15.3	2.34
TAMs/A360V	369 ± 137	3.54	63.1 ± 49.9	3.36
TAMs/N348I	919 ± 13.0	8.84	83.6 ± 38.9	4.45
TAMs/A360V/N348I	>1000	⋙	128 ± 94.7	6.81

[a] FC, -fold change in $K_{d(\text{RNase H})}$ value of each mutant RT was compared with that of WT RT.

TABLE 3
Polymerase-based K_d values

RT enzyme	15-bp hybrid duplex	
	$K_{d(\text{pol})}$	FC[a]
	nM	*-fold*
WT	12.8 ± 2.38	
TAMs	22.7 ± 3.31	1.77
TAMs/A360V	10.5 ± 1.87	0.820
TAMs/N348I	21.7 ± 1.05	1.69
TAMs/A360V/N348I	11.2 ± 3.29	0.875

[a] FC, -fold change in $K_{d(\text{pol})}$ value of each mutant RT was compared with that of WT RT.

These results raise the question of whether connection domain mutations may likewise affect binding in the context of polymerase- or excision-competent complexes. Diminished binding would compromise nucleotide incorporation and its excision, which is counterintuitive given the role of these mutations in AZT resistance. Excision of AZT-MP is generally inefficient and therefore difficult to measure under single turnover conditions. Thus, we made use of nucleotide incorporation events as a read-out to study binding in the polymerase/excision-competent complex. We utilized a 15-bp hybrid substrate that becomes extended to a 16-bp hybrid following nucleotide incorporation. WT and mutant RT enzymes show $K_{d(\text{pol})}$ values in a close range between 10 and 25 nM (Table 3). TAMs containing RT show a 2-fold increase in $K_{d(\text{pol})}$ when compared with WT RT. A360V appears to compensate for this deficit, whereas N348I shows no significant effect on substrate binding in this context. $K_{d(\text{pol})}$ values are at least an order of magnitude lower than $K_{d(\text{RNase H})}$ values, which confirms that the loss of contacts with the polymerase domain diminishes substrate binding in the RNase H-competent binding mode. Connection domain mutations appear to amplify these effects and cause substrate dissociation selectively from the RNase H-competent conformation.

Effect of N348I and A360V on HIV-1 RT Processivity—Differences in substrate binding in polymerase-competent complexes are generally low, although A360V appears to correct for the modest deficiency of TAMs. Such subtle differences in substrate binding, measured at a single primer-template position, may translate to differences in processive DNA synthesis that is monitored over multiple positions. To address this question, we compared DNA synthesis with the long RNA template under single turnover conditions in the absence of inhibitors. TAMs showed reduced full-length product formation under these conditions when compared with WT RT (Fig. 6). Processive DNA synthesis is then increased in the following order: TAMs/A360V < TAMs/N348I < TAMs/A360V/N348I. The latter mutant enzyme shows even higher levels of full-length product formation as compared with WT RT. Some pausing sites that occur toward the end of the template are more pronounced, with enzymes containing connection domain mutations. This observation shows that these enzymes produce more intermediate product; however, the complexes are likewise vulnerable to dissociation. To provide a measure for processive DNA synthesis, we have focused on the final product and compared the fraction of competent complexes between the different enzymes that have reached the end of the template (Table 4).

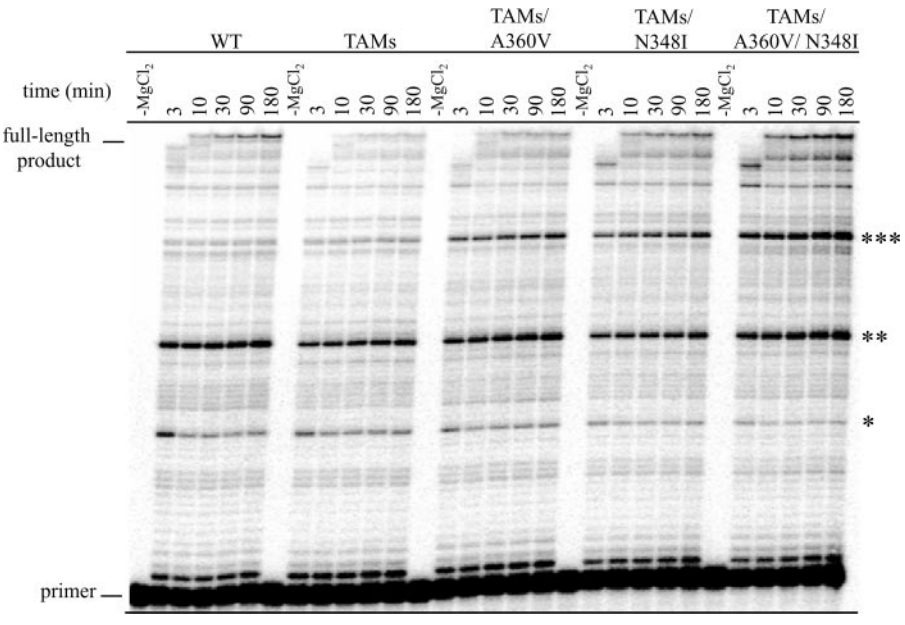

FIGURE 6. **The effect of connection domain mutations on processive DNA synthesis.** The long DNA·RNA substrate was incubated with each of the RT enzymes, and DNA elongation was initiated with the simultaneous addition of $MgCl_2$ and the heparin trap. Product formation was monitored over a time period ranging from 0 to 3 h, where the lower band is the primer and the highest band is the full-length product. Pausing sites are indicated by *asterisks*.

Thus, the subtle increases in substrate binding in the polymerase-

competent mode translate into increases in processive DNA synthesis with A360V-containing enzymes. Unexpectedly, N348I-containing enzymes can likewise increase processive DNA synthesis, although these enzymes do not appear to increase nucleic acid binding in this context.

N348I Increases PP_i-mediated Excision of AZT-MP—At this point, our data show that both factors (i) reduced RNase H activity and (ii) increased processivity correlate with increases in ATP-dependent excision of AZT-MP and rescue of DNA synthesis when TAMs and connection domain mutations are combined. Reductions in RNase H cleavage and increases in processive DNA synthesis affect the excision reaction indirectly. Diminished RNase H activity provides more time for excision to occur, and increases in processive DNA synthesis can compensate for the low rates associated with this reaction. Thus, increases in excision and rescue of DNA synthesis may be seen independently of the nature of the PP_i donor. To test this hypothesis, we studied the effects of the various mutant enzymes on PP_i-mediated excision of AZT-MP and the ensuing rescue of DNA synthesis. PP_i was used at physiologically relevant concentrations of 50 μM PP_i (Fig. 7). The RT enzymes containing TAMs alone or TAMs/A360V did not show significant differences in full-length product formation. However, marked increases in AZT-MP excision and rescue of DNA synthesis with TAMs/N348I and TAMs/A360V/N348I were observed. To test whether these effects can be seen independently of TAMs, which do not appear to improve binding and usage of PP_i (21), we conducted the same experiment with the single mutations A360V and N348I, respectively. Our data show that the N348I mutant confers increases in PP_i-mediated rescue of AZT-terminated DNA synthesis when compared with WT RT and TAMs (supplemental Fig. S5). The effects of A360V are by far not as pronounced as seen with N348I.

Connection Domain Mutations Can Increase AZT-MP Excision Independently of RNase H Activity—Finally, we studied whether increases in processive DNA synthesis may be sufficient to increase levels of rescue of DNA synthesis. To address this, we introduced the RNase H-negative E478Q mutation (48) against a background of TAMs and TAMs/A360V/N348I. The latter shows the strongest effects with regard to increases in processive DNA synthesis, increases in AZT-MP excision, and decreases in RNase H activity. When comparing TAMs with TAMs/E478Q, we observed increases in ATP-dependent rescue of AZT-terminated DNA synthesis (Fig. 8). We obtained essentially the same results with PP_i as the substrate for excision (supplemental Fig. S6). Also, the same effect is seen when comparing TAMs/A360V/N348I with TAMs/A360V/N348I/E478Q, which shows that the loss of RNase H activity enhances the rescue reaction. In addition, the comparison of TAMs/A360V/N348I/E478Q with TAMs/E478Q points to a strong RNase H-independent component. Formation of the full-length product is much higher with TAMs/A360V/N348I/E478Q, which shows that the contribution to increases in rescue of DNA synthesis is in part RNase H-independent.

TABLE 4
Processivity values

Enzyme	Processive complex[a]
	%
WT	2.77
TAMs	2.09
TAMs/A360V	3.00
TAMs/N348I	5.36
TAMs/A360V/N348I	6.36

[a] Enzyme processivity is expressed as "percentage of processive complex" as described under "Experimental Procedures."

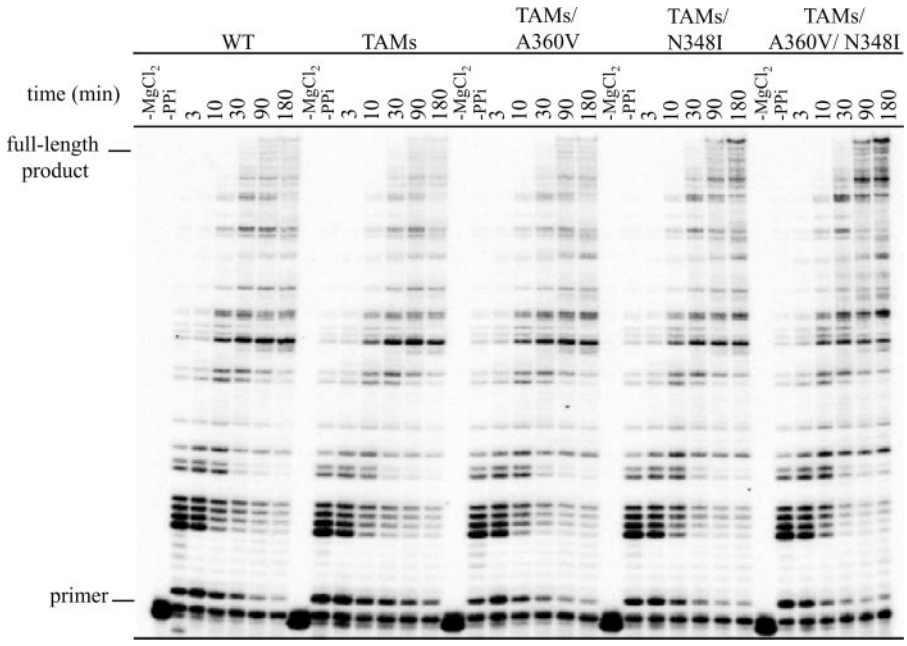

FIGURE 7. **PP_i-mediated multisite excision of AZT-MP on the DNA·RNA nucleic acid substrate.** DNA synthesis rescue was monitored over time in the presence of AZT and PP_i for each of the RT enzymes (WT, TAMs, TAMs/A360V, TAMs/N348I, and TAMs/A360V/N348I, respectively) up to 3 h at 37 °C (time points indicated). Product formation was visualized on a denaturing polyacrylamide gel, where the lowest band is the radiolabeled DNA primer and the highest band is the full-length DNA product. The negative PP_i *control lane* shows polymerization in the absence of PP_i-mediated DNA synthesis rescue.

DISCUSSION

Connection domain mutations N348I and A360V in HIV-1 RT can contribute to increases in AZT resistance. Both mutations have been identified in clinical samples of treatment-experienced individuals (24–26, 33). Clinical data obtained from Canadian (26) (this study) and Brazilian cohorts (25) suggest that N348I can appear early in therapy, independently of preselected TAMs, whereas A360V appears late following the emergence of TAMs. It has been proposed that connection domain mutations exert their effects on excision indirectly through alterations in RNase H cleavage (26, 28, 32, 33). Here we asked how the two connection domain mutations can affect RNase H cleavage and whether such changes are necessary and sufficient to cause an increase in phosphorolytic excision of AZT-MP. Our biochemi-

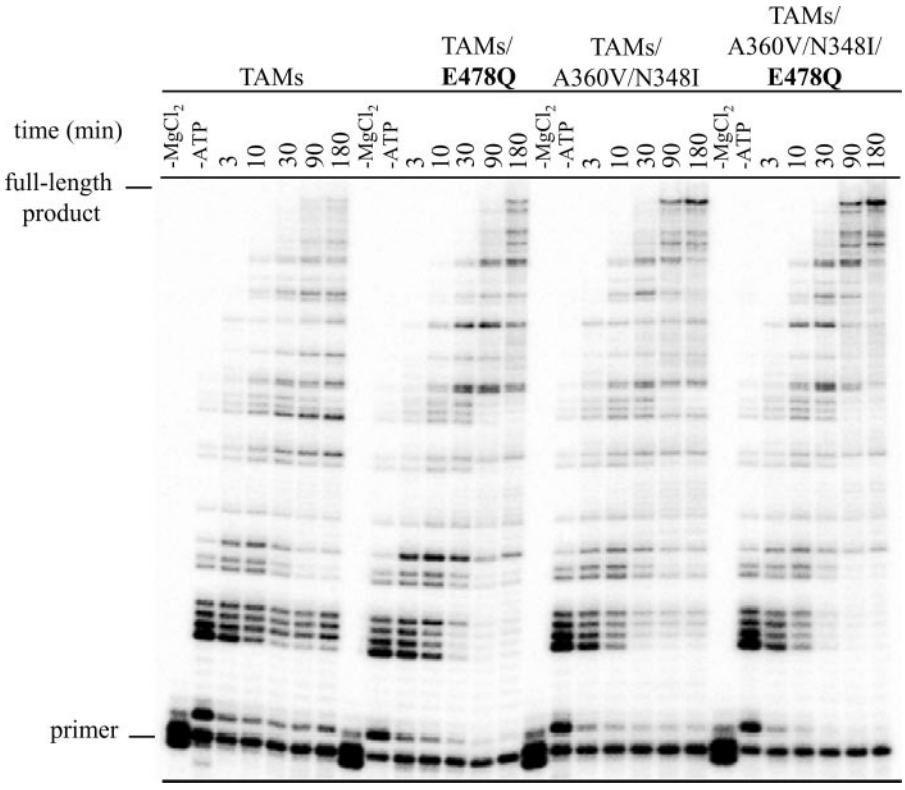

FIGURE 8. **RNase H-independent ATP-mediated AZT-MP excision on the DNA·RNA substrate.** DNA synthesis and ATP-mediated AZT-MP excision were monitored with enzymes containing the E478Q mutation (TAMs, TAMs/E478Q, TAMs/A360V/N348I, and TAMs/A360V/N348I/E478Q, respectively). Product formation was visualized on a denaturing polyacrylamide gel, where the *lowest band* is the radiolabeled DNA primer and the *highest band* is the full-length DNA product.

cal studies provide strong evidence for a mechanism that involves both RNase H-dependent and -independent contributions to increases in AZT-MP excision and, in turn, resistance to this drug (Fig. 9).

Effects of Connection Domain Mutations on RNase H-competent Complexes—Band shift experiments under nondenaturing conditions demonstrate that RNase H cleavage will ultimately cause the release of the primer from complexes with WT RT that progressively degrade the template strand. The TAMs/A360V/N348I mutant that is severely compromised in RNase H activity delays the release of the primer. These findings support the notion that RNase H cleavage can limit the available time for excision to occur, and mutant enzymes with diminished RNase H activity confer an advantage in this regard (32). Transiently formed hybrids become detectable with the mutant enzyme, suggesting that the release of the primer is a two-step process that follows dissociation of shorter DNA·RNA hybrids (Fig. 9, *steps 1* and *2*). Binding studies reveal that TAMs and the two connection domain mutations reduce binding of DNA·RNA substrates when binding is monitored through RNase H cleavage. This effect is amplified as the nucleic acid substrates get shorter, which helps to explain why transiently formed hybrids become detectable with the TAMs/A360V/N348I mutant.

Substrate binding follows the order WT RT > TAMs > TAMs/A360V > TAMs/N348I > TAMs/A360V/N348I, which correlates directly with RNase H activity measurements in time course experiments. Thus, diminished RNase H cleavage, including both primary and secondary cuts, is caused by diminished substrate binding in RNase H-competent complexes (Fig. 9, *step 1*).

Effects of Connection Domain Mutations on Polymerase-competent Complexes—Recent studies have shown that excision can only occur in a pretranslocated complex, whereas nucleotide incorporation can only occur in a post-translocated complex (49–53). Both configurations exist in a dynamic equilibrium (37, 50, 53–56). TAMs show a subtle bias toward pretranslocation; however, the two connection domain mutations do not appear to influence this equilibrium (data not shown). Hence, the efficiency of substrate binding in polymerase- and excision-competent complexes can be assayed through nucleotide incorporation events. This approach revealed that substrate binding is significantly enhanced in this conformation and that the mutational background appears to be of minor importance in this regard. $K_{d(\mathrm{pol})}$ values for polymerase-competent complexes range between 10 and 25 nM, whereas $K_{d(\mathrm{RNase\ H})}$ values for RNase H-competent complexes range between 100 and >1000 nM. Most contacts between RT and its nucleic acid substrate are located in close proximity to the polymerase active site, the template 5′-overhang, and the first 10 bp of the nucleic acid substrate (1, 12, 57). These interactions are lost as the substrate shortens due to RNA template cleavage in the RNase H-competent binding mode. Binding of transiently formed substrates is therefore inferior in this configuration, and the connection domain mutations amplify this effect.

The TAM-containing mutant shows small, 2-fold decreases in substrate binding in both polymerase- and RNase H-competent binding modes relative to WT. In contrast, the connection domain mutations promote dissociation selectively in the RNase H-competent mode. Binding in the polymerase-competent mode is either not further affected with enzymes containing N348I or modestly enhanced with enzymes containing A360V. A360V appears to compensate for the deficit introduced by TAMs, which helps to explain why this mutation is generally detected late following the emergence of classic TAMs (Fig. 9, *step 3*).

Structural Interpretation—The aforementioned results raise the question of how the two connection mutations N348I and A360V affect specifically the RNase H-competent complex. Crystal structures of RT with DNA·DNA (12) or DNA·RNA (34) substrates show residue Asn^{348} in close proximity to but not in contact with the primer between positions −3 and −5. Thus, the N348I mutation in p66 may affect substrate binding

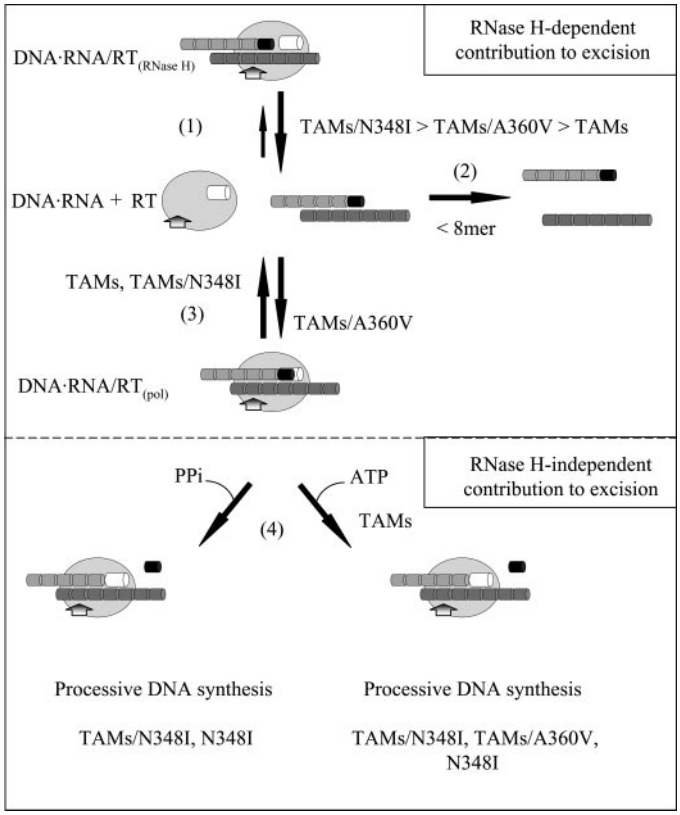

FIGURE 9. **Proposed mechanisms for contributions of A360V and N348I to increases in excision and rescue of AZT-terminated DNA synthesis.** RT enzyme is depicted as the *oval shape* containing the RNase H domain (*arrow*) and polymerase domain (*white cylinder*). The nucleic acid substrate consists of the RNA template (*dark gray cylinder*) and DNA primer (*light gray cylinder*) with the AZT chain terminator at the 3′ terminus (*black cylinder*). In *step 1*, mutations N348I, A360V, and TAMs promote the dissociation of the RNase H-competent complex (DNA·RNA·$RT_{(RNase\ H)}$) from the nucleic acid substrate. If the double-stranded region of the nucleic acid substrate is less than 8 bp, the DNA·RNA substrate dissociates, and no excision can occur (*step 2*). Once dissociated, the enzyme can reassociate with the substrate and form a polymerase-competent complex (DNA·RNA·$RT_{(pol)}$) (*step 3*). TAMs RT shows a deficit in binding the substrate in this mode, whereas TAMs/A360V facilitates binding. *Step 4* represents enzyme processivity and AZT-MP excision (see "Discussion").

indirectly (23). Long range effects on RNase H cleavage are plausible, given that NNRTIs were also shown to affect RNase H activity (58, 59). However, the selective diminution in substrate binding in RNase H-competent complexes suggests a possible role for N348I in p51, which is found within 16 Å between positions −15 and −16 of the primer.

Ala^{360} in p66 is 5 Å away from positions −12 and −13 of the DNA primer. The bulkier side chain of A360V may therefore influence the proper positioning of the primer to the RNase H active site. Such steric problems may specifically affect the RNase H-competent complex, because the natural residue is part of the RNase H primer grip that helps position the substrate at the RNase H active site. Moreover, the loss of important contacts through the polymerase domain has already destabilized the RNase H-competent complex with shorter substrates. In contrast, interactions with the polymerase domain may neutralize any unfavorable contacts with the connection domain in the context of a polymerase-dependent complex. Subtle increases in substrate binding with A360V may be attributable to additional contacts with the longer side chain. Such effects may also depend on the nature of the nucleic acid substrate, which helps to explain why connection domain mutations do not appear to increase excision on DNA·DNA (26). Crystallographic data are required to address these hypotheses.

Consequences for Excision of AZT-MP—The selective dissociation from RNase H-competent complexes provides a plausible mechanism that links a reduction in RNase H activity to increases in the efficiency of AZT-MP excision. The deficit in RNase H cleavage associated with TAMs appears insignificant and is presumably neutralized by deficits in binding to the polymerase-competent mode. If the diminished RNase H activity were to play a role in increases in excision, one would expect to detect higher levels of excision independently of the nature of the PP_i donor. Accordingly, in contrast to TAMs, which only show increased excision when ATP is the PP_i donor, the addition of A360V and/or N348I against a background of TAMs increases the efficiency of AZT-MP excision with both PP_i and ATP.

The ability to recruit PP_i is potentially relevant in biological settings, given that rates of PP_i-mediated excision are much higher than rates of ATP-dependent reactions (60). N348I shows the strongest effects in this regard. This is seen in the presence and absence of TAMs, which helps to explain why N348I often emerges early after initiation of therapy before the selection of classic TAMs.

RNase H-independent Contribution to Excision—Despite the mechanistic link between diminished RNase H cleavage and increases in excision, our results point to an additional, RNase H-independent contribution to AZT resistance by N348I and A360V. The TAMs/A360V/N348I mutant is still more efficient in AZT-MP excision and rescue of DNA synthesis as compared with TAMs when both enzymes contain the RNase H-negative E478Q mutation. Increases in processive DNA synthesis associated with TAMs/A360V and TAMs/N348I appear to account for this effect (Fig. 9, *step 4*). The moderate increases in binding in the polymerase-competent mode with A360V provide a plausible mechanism that can translate into both increases in excision and the ensuing rescue reaction. In contrast, N348I does not appear to exert its effects through differences in nucleic acid binding. It is therefore conceivable that this mutation can also affect the structure around the polymerase active site and, in turn, nucleotide binding and/or excision.

Collectively, our data show that connection domain mutations increase efficiency of AZT-MP excision through both RNase H-dependent and -independent mechanisms. Both the selective dissociation from RNase H-competent complexes and increases in processive DNA synthesis have been identified as important parameters in this regard. The distinct, complementary mechanisms can potentially synergize and contribute to higher levels of excision of AZT, which can amplify resistance to this drug and compensate for deficiencies in viral fitness. These findings warrant clinical studies that assess potential beneficial effects in the management of HIV infection when including these mutations in routine genotypic testing.

Acknowledgments—We thank Mia J. Biondi for carefully reading the manuscript and Colins E. Vasquez for software expertise.

REFERENCES

1. Jacobo-Molina, A., Ding, J., Nanni, R. G., Clark, A. D., Jr., Lu, X., Tantillo, C., Williams, R. L., Kamer, G., Ferris, A. L., Clark, P., Hizi, A., Hughes, S. H., and Arnold, E. (1993) *Proc. Natl. Acad. Sci. U. S. A.* **90,** 6320–6324
2. Kohlstaedt, L. A., Wang, J., Friedman, J. M., Rice, P. A., and Steitz, T. A. (1992) *Science* **256,** 1783–1790
3. Schultz, S. J., and Champoux, J. J. (2008) *Virus Res.* **134,** 86–103
4. De Clercq, E. (2007) *Verh. K Acad. Geneeskd Belg.* **69,** 81–104
5. Ilina, T., and Parniak, M. A. (2008) *Adv. Pharmacol.* **56,** 121–167
6. El Safadi, Y., Vivet-Boudou, V., and Marquet, R. (2007) *Appl. Microbiol. Biotechnol.* **75,** 723–737
7. Basavapathruni, A., and Anderson, K. S. (2006) *Curr. Pharm. Des.* **12,** 1857–1865
8. Sluis-Cremer, N., and Tachedjian, G. (2008) *Virus Res.* **134,** 147–156
9. Cingolani, A., Antinori, A., Rizzo, M. G., Murri, R., Ammassari, A., Baldini, F., Di Giambenedetto, S., Cauda, R., and De Luca, A. (2002) *AIDS* **16,** 369–379
10. Tural, C., Ruiz, L., Holtzer, C., Schapiro, J., Viciana, P., Gonzalez, J., Domingo, P., Boucher, C., Rey-Joly, C., and Clotet, B. (2002) *AIDS* **16,** 209–218
11. Zolopa, A. R., Lazzeroni, L. C., Rinehart, A., Vezinet, F. B., Clavel, F., Collier, A., Conway, B., Gulick, R. M., Holodniy, M., Perno, C. F., Shafer, R. W., Richman, D. D., Wainberg, M. A., and Kuritzkes, D. R. (2005) *Clin. Infect. Dis.* **41,** 92–99
12. Huang, H., Chopra, R., Verdine, G. L., and Harrison, S. C. (1998) *Science* **282,** 1669–1675
13. Ren, J., and Stammers, D. K. (2005) *Trends Pharmacol. Sci.* **26,** 4–7
14. Sarafianos, S. G., Das, K., Ding, J., Boyer, P. L., Hughes, S. H., and Arnold, E. (1999) *Chem. Biol.* **6,** R137–146
15. Johnson, V. A., Brun-Vezinet, F., Clotet, B., Gunthard, H. F., Kuritzkes, D. R., Pillay, D., Schapiro, J. M., and Richman, D. D. (2008) *Top. HIV Med.* **16,** 62–68
16. Goldschmidt, V., and Marquet, R. (2004) *Int. J. Biochem. Cell Biol.* **36,** 1687–1705
17. Menendez-Arias, L. (2008) *Virus Res.* **134,** 124–146
18. Gotte, M. (2004) *Expert Rev. Anti-Infect. Ther.* **2,** 707–716
19. Meyer, P. R., Matsuura, S. E., Mian, A. M., So, A. G., and Scott, W. A. (1999) *Mol. Cell* **4,** 35–43
20. Meyer, P. R., Matsuura, S. E., Tolun, A. A., Pfeifer, I., So, A. G., Mellors, J. W., and Scott, W. A. (2002) *Antimicrob. Agents Chemother.* **46,** 1540–1545
21. Ray, A. S., Murakami, E., Basavapathruni, A., Vaccaro, J. A., Ulrich, D., Chu, C. K., Schinazi, R. F., and Anderson, K. S. (2003) *Biochemistry* **42,** 8831–8841
22. Gotte, M. (2007) *PLoS Med.* **4,** e346
23. Hachiya, A., Kodama, E. N., Sarafianos, S. G., Schuckmann, M. M., Sakagami, Y., Matsuoka, M., Takiguchi, M., Gatanaga, H., and Oka, S. (2008) *J. Virol.* **82,** 3261–3270
24. Ntemgwa, M., Wainberg, M. A., Oliveira, M., Moisi, D., Lalonde, R., Micheli, V., and Brenner, B. G. (2007) *Antimicrob. Agents Chemother.* **51,** 3861–3869
25. Santos, A. F., Lengruber, R. B., Soares, E. A., Jere, A., Sprinz, E., Martinez, A. M., Silveira, J., Sion, F. S., Pathak, V. K., and Soares, M. A. (2008) *PLoS ONE* **3,** e1781
26. Yap, S. H., Sheen, C. W., Fahey, J., Zanin, M., Tyssen, D., Lima, V. D., Wynhoven, B., Kuiper, M., Sluis-Cremer, N., Harrigan, P. R., and Tachedjian, G. (2007) *PLoS Med.* **4,** 1887–1900
27. Cane, P. A., Green, H., Fearnhill, E., and Dunn, D. (2007) *AIDS* **21,** 447–455
28. Brehm, J. H., Koontz, D., Meteer, J. D., Pathak, V., Sluis-Cremer, N., and Mellors, J. W. (2007) *J. Virol.* **81,** 7852–7859
29. Zelina, S., Sheen, C. W., Radzio, J., Mellors, J. W., and Sluis-Cremer, N. (2008) *Antimicrob. Agents Chemother.* **52,** 157–163
30. Kemp, S. D., Shi, C., Bloor, S., Harrigan, P. R., Mellors, J. W., and Larder, B. A. (1998) *J. Virol.* **72,** 5093–5098
31. Harrigan, P. R., Salim, M., Stammers, D. K., Wynhoven, B., Brumme, Z. L., McKenna, P., Larder, B., and Kemp, S. D. (2002) *J. Virol.* **76,** 6836–6840
32. Nikolenko, G. N., Palmer, S., Maldarelli, F., Mellors, J. W., Coffin, J. M., and Pathak, V. K. (2005) *Proc. Natl. Acad. Sci. U. S. A.* **102,** 2093–2098
33. Nikolenko, G. N., Delviks-Frankenberry, K. A., Palmer, S., Maldarelli, F., Fivash, M. J., Jr., Coffin, J. M., and Pathak, V. K. (2007) *Proc. Natl. Acad. Sci. U. S. A.* **104,** 317–322
34. Sarafianos, S. G., Das, K., Tantillo, C., Clark, A. D., Jr., Ding, J., Whitcomb, J. M., Boyer, P. L., Hughes, S. H., and Arnold, E. (2001) *EMBO J.* **20,** 1449–1461
35. Le Grice, S. F., and Gruninger-Leitch, F. (1990) *Eur. J. Biochem.* **187,** 307–314
36. Arts, E. J., Li, X., Gu, Z., Kleiman, L., Parniak, M. A., and Wainberg, M. A. (1994) *J. Biol. Chem.* **269,** 14672–14680
37. Marchand, B., and Gotte, M. (2003) *J. Biol. Chem.* **278,** 35362–35372
38. Gotte, M., Arion, D., Parniak, M. A., and Wainberg, M. A. (2000) *J. Virol.* **74,** 3579–3585
39. Kati, W. M., Johnson, K. A., Jerva, L. F., and Anderson, K. S. (1992) *J. Biol. Chem.* **267,** 25988–25997
40. Lanchy, J. M., Ehresmann, C., Le Grice, S. F., Ehresmann, B., and Marquet, R. (1996) *EMBO J.* **15,** 7178–7187
41. Schatz, O., Mous, J., and Le Grice, S. F. (1990) *EMBO J.* **9,** 1171–1176
42. Gotte, M., Fackler, S., Hermann, T., Perola, E., Cellai, L., Gross, H. J., Le Grice, S. F., and Heumann, H. (1995) *EMBO J.* **14,** 833–841
43. Furfine, E. S., and Reardon, J. E. (1991) *J. Biol. Chem.* **266,** 406–412
44. Gopalakrishnan, V., Peliska, J. A., and Benkovic, S. J. (1992) *Proc. Natl. Acad. Sci. U. S. A.* **89,** 10763–10767
45. Gotte, M., Maier, G., Gross, H. J., and Heumann, H. (1998) *J. Biol. Chem.* **273,** 10139–10146
46. Tong, W., Lu, C. D., Sharma, S. K., Matsuura, S., So, A. G., and Scott, W. A. (1997) *Biochemistry* **36,** 5749–5757
47. Meyer, P. R., Matsuura, S. E., Schinazi, R. F., So, A. G., and Scott, W. A. (2000) *Antimicrob. Agents Chemother.* **44,** 3465–3472
48. Cristofaro, J. V., Rausch, J. W., Le Grice, S. F., and DeStefano, J. J. (2002) *Biochemistry* **41,** 10968–10975
49. Boyer, P. L., Sarafianos, S. G., Arnold, E., and Hughes, S. H. (2001) *J. Virol.* **75,** 4832–4842
50. Marchand, B., White, K. L., Ly, J. K., Margot, N. A., Wang, R., McDermott, M., Miller, M. D., and Gotte, M. (2007) *Antimicrob. Agents Chemother.* **51,** 2911–2919
51. Sarafianos, S. G., Clark, A. D., Jr., Das, K., Tuske, S., Birktoft, J. J., Ilankumaran, P., Ramesha, A. R., Sayer, J. M., Jerina, D. M., Boyer, P. L., Hughes, S. H., and Arnold, E. (2002) *EMBO J.* **21,** 6614–6624
52. Sarafianos, S. G., Clark, A. D., Jr., Tuske, S., Squire, C. J., Das, K., Sheng, D., Ilankumaran, P., Ramesha, A. R., Kroth, H., Sayer, J. M., Jerina, D. M., Boyer, P. L., Hughes, S. H., and Arnold, E. (2003) *J. Biol. Chem.* **278,** 16280–16288
53. Marchand, B., and Gotte, M. (2004) *Int. J. Biochem. Cell Biol.* **36,** 1823–1835
54. Gotte, M. (2006) *Curr. Pharm. Des.* **12,** 1867–1877
55. Marchand, B., Tchesnokov, E. P., and Gotte, M. (2007) *J. Biol. Chem.* **282,** 3337–3346
56. Meyer, P. R., Rutvisuttinunt, W., Matsuura, S. E., So, A. G., and Scott, W. A. (2007) *J. Mol. Biol.* **369,** 41–54
57. Ding, J., Das, K., Hsiou, Y., Sarafianos, S. G., Clark, A. D., Jr., Jacobo-Molina, A., Tantillo, C., Hughes, S. H., and Arnold, E. (1998) *J. Mol. Biol.* **284,** 1095–1111
58. Radzio, J., and Sluis-Cremer, N. (2008) *Mol. Pharmacol.* **73,** 601–606
59. Palaniappan, C., Wisniewski, M., Jacques, P. S., Le Grice, S. F., Fay, P. J., and Bambara, R. A. (1997) *J. Biol. Chem.* **272,** 11157–11164
60. Smith, A. J., and Scott, W. A. (2006) *Curr. Pharm. Des.* **12,** 1827–1841